Sustainable Energy & Fuels

ROYAL SOCIETY OF CHEMISTRY

PAPER

View Article Online
View Journal | View Issue

Cite this: *Sustainable Energy Fuels*, 2025, **9**, 4041

Remarkable power factor improvement in a porous, nanostructured thermoelectric oxide functionalized with viologen molecules†

M. M. Rahman, L. Márquez-García, M. Solis-de la Fuente and J. García-Cañadas *

Thermoelectric (TE) materials are attractive as a technology able to directly convert heat into electricity. Most of the successful strategies to improve TE performance are based on decreasing the thermal conductivity, while approaches aiming at increasing the power factor (PF = σS^2, where σ is the electrical conductivity and S the Seebeck coefficient) have been limited. Here, we introduce a new strategy to significantly improve this parameter by using a porous, nanostructured TE solid (Sb-doped SnO_2) functionalized with a redox molecule: bis-(2-phosphonoethyl)-4,4′-bipyridinium dichloride. We found that, after functionalization, a 50% average reduction in the electrical resistivity, with a small increase of 9% in the absolute value of the Seebeck coefficient, takes place, leading to a remarkable 2.5 times PF improvement. In order to explain the effects observed, impedance spectroscopy measurements were performed, concluding that the electrical resistivity decrease is produced by the donation of electrons from the redox molecules into the oxide material. This new strategy remarkably achieves a substantial decrease in electrical resistivity without a Seebeck coefficient reduction (there is even a small increase), which is highly beneficial and not usually common, demonstrating a high potential to increase the PF.

Received 15th April 2025
Accepted 31st May 2025

DOI: 10.1039/d5se00538h

rsc.li/sustainable-energy

1. Introduction

More than 60% of the energy used globally is lost as waste heat that is released into the atmosphere without being utilized.[1] Apart from this, many heat sources are widely available, such as the sun and our own bodies. Thermoelectric (TE) devices allow the direct conversion of heat into electricity, and *vice versa*, under silent, reliable, secure and eco-friendly conditions.[2,3] They can be used in radioisotope TE generators for spacecrafts, as solar TE generators, in vehicles and industries utilizing heat from hot exhaust gases and refrigeration circuits, and to power wearable devices and sensors, among other applications.[4,5]

However, the widespread application of TE materials for energy harvesting is mainly limited by their low conversion efficiencies. Generally, the TE performance of a material is assessed by its dimensionless figure of merit $ZT = S^2\sigma T/\kappa$, where S, σ, κ, and T represent the Seebeck coefficient, the electrical conductivity, the thermal conductivity, and the absolute temperature, respectively. The term $S^2\sigma$ is known as the power factor (PF). Most of the existing performance improvement strategies are based on introducing modifications within the material lattice (*e.g.* doping, grain boundary and defect engineering, nanostructuring, *etc.*), which have mainly achieved a reduction of the thermal conductivity.[6] In contrast, strategies to improve the PF have been limited, and involve the difficult task of decoupling the Seebeck coefficient from the electrical conductivity.[7]

Here, we introduce a new strategy to improve the TE PF which is not based on producing modifications in the material lattice, but on acting on the material surface. In this way, this new approach involves functionalizing the surface of a porous, nanostructured material by covalently attaching redox molecules to its surface. To evaluate the potential of this strategy, a porous, nanostructured Sb-doped SnO_2 film was employed, which provides a large surface area for functionalization. Although it is a material with modest TE properties, it is easy to prepare and possesses the morphology needed.[8,9] As a redox molecule, bis-(2-phosphonoethyl)-4,4′-bipyridinium dichloride, which belongs to the family of viologen compounds, was used. This molecule is typically used to functionalize electrodes in fields such as electrochromics.[10,11] A viologen can offer three different redox states, as shown in Fig. 1.

In our study, we investigate the effect of the functionalization on the PF of the Sb:SnO_2 film, identifying remarkable PF improvements. By using impedance spectroscopy, we identify the mechanisms behind the improvements observed. Our results establish this new strategy as a PF enhancement route that can be possibly extended to other materials.

Department of Industrial Systems Engineering and Design, Universitat Jaume I, Av. Vicent Sos Baynat s/n, 12006 Castelló de la Plana, Spain. E-mail: garciaj@uji.es

† Electronic supplementary information (ESI) available. See DOI: https://doi.org/10.1039/d5se00538h

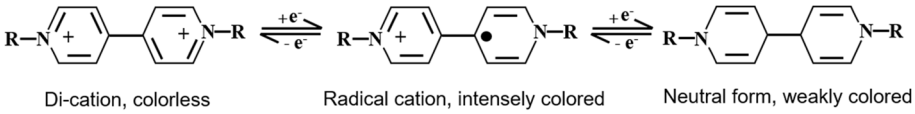

Fig. 1 Redox states of a viologen molecule.

2. Experimental section

Film preparation

Porous, nanostructured Sb:SnO_2 films were deposited on soda-lime glass substrates of 25 mm × 15 mm size with a 1.8 mm thickness. Before the film deposition, the substrates were cleaned by following three sonication steps, each lasting 15 min, in different media. First, sonication was carried out in a soap (Labkem, SOAP-0685K0)/water solution (1 : 10 v/v). The second sonication step involved using distilled water to remove any residual soap, and the final step involved sonication in isopropanol (Labkem, PROL-P0P-5K0). The substrates were then dried completely under compressed air flow, and treated in a UV/ozone cleaner (Ossila, L2002A2-UK) for 20 min. Afterwards, four layers of a commercially available colloidal aqueous dispersion of Sb:SnO_2 (Keeling & Walker, A20W) were deposited by spin coating (Laurell, WS-650MZ-23NPPB) at 2500 rpm for 15 s, covering a centered area of the substrate of 10 mm × 5 mm, which was obtained by masking with Magic Scotch tape. Films were dried after each deposition on a hot plate at 100 °C for 10 min and subsequently cooled down in air for 10 min. Finally, the films were heated at 550 °C for 45 min in a furnace (Nabertherm, 400-1) at a 3 °C min^{-1} heating rate. Scanning electron microscopy (SEM) images of the films were obtained using a JEOL 7001F instrument (Oxford Instruments).

Functionalization

Pt contacts were deposited at both ends of the films by sputtering deposition (Quorum, Q300T D Plus) for 60 s, following the initial deposition of a Cr seeding layer for 15 s (see Fig. 2a). The viologen redox molecule bis-(2-phosphonoethyl)-4,4′-bipyridinium dichloride was synthesized as previously described.[12] For the functionalization, a 0.5 mM viologen solution in methanol (≥99.8%, VWR Chemicals) was prepared. The functionalization of 3 samples (S1 to S3) was achieved by first heating the Sb:SnO_2 films at 100 °C for 10 min, allowing them to cool down, and finally, immediately after cooling, immersing them in the prepared viologen solution overnight. Once removed from the viologen solution, the films were rinsed with methanol and dried in air overnight. A fourth sample (S4) was prepared using the same process, but employing a solution with only methanol (no viologen). This is in order to evaluate if methanol produces some effect.

TE measurements

Seebeck coefficient and electrical resistance measurements were carried out in a homemade setup. In this setup, two copper blocks were used to create a temperature difference, as shown in Fig. 2b. A copper block with 30 mm × 30 mm × 10 mm dimensions and three cartridge heaters inserted (Watlow, ref.

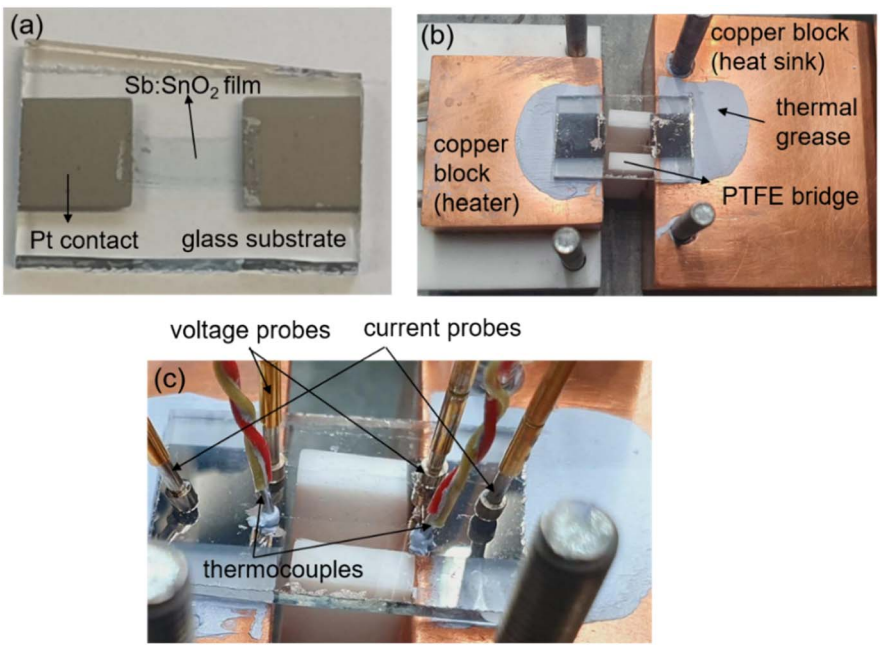

Fig. 2 Images of (a) one of the films prepared, (b) a sample placed on top of the two Cu blocks connected by a PTFE bridge, and (c) a sample in the setup contacted by different probes and thermocouples.

C1E13-L12) served as the heat source. Another copper block, with 50 mm × 50 mm × 30 mm dimensions, was used as the heat sink. The prepared films were positioned on top of the copper blocks establishing a hot and cold side, as shown in Fig. 2b. Both copper blocks were separated by a polytetrafluoroethylene (PTFE) bridge. Thermal grease (RS, ref. 2173835) was applied at the glass/copper interfaces to enhance the thermal contact and improve heat transfer.

To measure the Seebeck coefficient, the temperature difference was monitored using two K-type thermocouples (RS, ref. 8140134) placed on top of the glass substrate near the ends of the film (see Fig. 2c) with a small amount of thermal grease at their tips to improve the thermal contact. Two spring probes (RS, ref. 2615092) were positioned on top of the glass substrate, close to the contact surface of Pt and the oxide film at each side, to perform the open-circuit voltage measurements (see Fig. 2c). Seebeck coefficient values were obtained from the slope of the open-circuit voltage V_{oc} *versus* the temperature difference ΔT curves. The V_{oc} was measured with a Keithley 2182A nanovoltmeter. The error of the Seebeck coefficient measurements, obtained from the error provided by the linear fitting, was below 4%.

To measure the electrical resistance, the same probes used to measure V_{oc} above were used to measure the voltage. In addition, two more spring probes were positioned on the edge of the Pt contacts at each side to measure the current (see Fig. 2c). The electrical resistance was obtained from the slope of current–voltage (I–V) curves at no temperature difference using a Keithley 2450 source meter, scanning the current with a delay time of 1 ms. The error of the electrical resistance measurements, obtained from the linear fitting of the I–V curve, was below 2%. All electrical measurements were taken with coaxial cables to minimize electrical interference from the surroundings.

Electrochemical measurements

Impedance spectroscopy measurements of the films were also performed using the same configuration of the probes as for the electrical resistance determination described above and under $\Delta T = 0$ K. Measurements were conducted in potentiostatic mode at 0 V dc voltage in the 0.01 Hz to 1 MHz frequency range and applying a 20 mV amplitude. Cyclic voltammetry measurements were performed in a standard 3-electrode cell at 10 mV s^{-1} scan rate. N_2 was bubbled through the electrolyte for 20 min before carrying out the experiments, and then a N_2 flow was maintained at the top of the cell throughout the experiments. A Pt sheet (Glentham Life Sciences, ref. GX2917) and a Ag wire (Alfa-Aesar, ref. 11469) were used as counter and pseudo reference electrodes, respectively. For these cyclic voltammetry measurements, a Sb:SnO_2 film deposited on a fluorine-doped tin oxide (FTO) glass substrate (Sigma Aldrich, ref. 735167-1EA), following the same procedure mentioned above, was used as the working electrode. In order to avoid the contact between the non-covered FTO surface and the electrolyte, Scotch Magic tape was used in this non-covered part to block the electrolyte access. A 0.1 M solution of tetrabutylammonium tetrafluroborate (Sigma Aldrich, ref. 217964) in 3-methoxypropionitrile (Sigma Aldrich, ref. 443778) was used as the electrolyte. A Metrohm-Autolab PGSTAT204 instrument equipped with a FRA32M frequency response analyzer was employed for both impedance and cyclic voltammetry measurements.

3. Results and discussion

Fig. 3 shows the SEM images of the Sb:SnO_2 films prepared before functionalization. It can be seen that the film consists of interconnected nanoparticles ranging in size from 6 to 10 nm. Moreover, the presence of pores in the 2–50 nm range is also observed, and the film thickness is approximately 1.0 μm, as

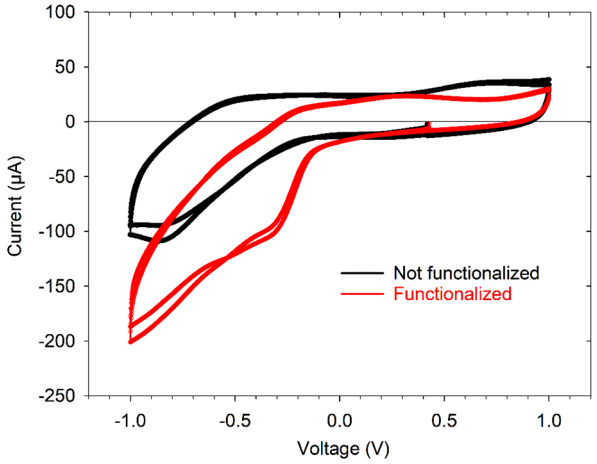

Fig. 4 Cyclic voltammograms of a functionalized and non-functionalized Sb:SnO_2 film.

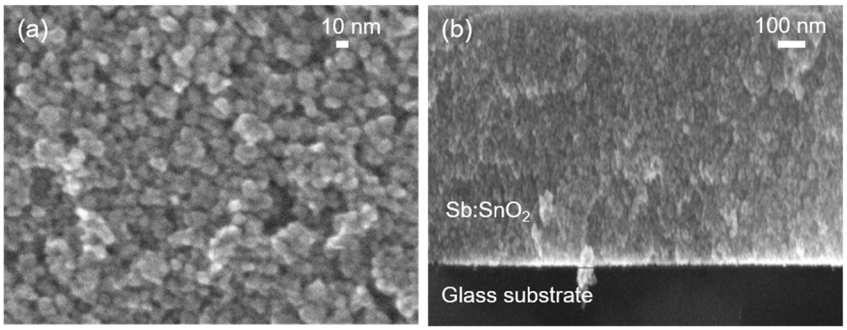

Fig. 3 (a) Top and (b) cross-sectional SEM images of a bare Sb-doped SnO_2 film.

Table 1 Seebeck coefficient and electrical resistance values, and their variations, for the Sb:SnO_2 films before and after their functionalization. The power factor ratio between functionalized and non-functionalized films is also given

	Seebeck coefficient ($\mu V\ K^{-1}$)			Electrical resistance (kΩ)			
Sample	Non-func.	Func.	Variation (%)	Non-func.	Func.	Variation (%)	PF_{func}/PF_{not}
S1	−33.12	−34.04	2.77	26.75	12.48	−53.32	2.26
S2	−43.87	−49.25	10.92	48.79	20.45	−58.08	3.01
S3	−40.05	−45.22	12.90	38.00	20.70	−45.52	2.34
S4	−44.88	−41.13	−8.33	16.21	14.74	−9.02	0.92

shown in Fig. 3b. It should be noted that the expected phase (cassiterite SnO_2) was previously identified by XRD experiments in a previous article.[9] Also, it can be seen in that reference that no changes in the XRD patterns were observed after the annealing process. In addition, an EDX analysis from the same article showed no changes in the chemical composition of the film after the thermal treatment.

In order to verify that the viologen molecules were successfully attached to the porous solid, cyclic voltammetry measurements were carried out, before and after the functionalization process, on the Sb:SnO_2 film deposited on FTO (see Fig. 4). It can be observed that the main difference between both voltammograms is the presence of a peak around −0.35 V in the functionalized sample, which is related to the reduction of the viologen molecules to their blue-colored redox form. In fact, the functionalized film turned from transparent to blue around that voltage.[10,12] This change in color was not observed in the non-functionalized film.

In order to evaluate the effect of the functionalization on the TE properties, the Seebeck coefficient and the film electrical resistance were measured for three Sb:SnO_2 samples (S1 to S3) before and after the functionalization process. Results are shown in Table 1 and Fig. S1, S2.† It can be observed that the absolute value of the Seebeck coefficient did not vary much after the functionalization process. It only experienced an 8.9% average increase. However, the electrical resistance R showed a remarkable decrease of 49.7% on average. This significant reduction of the resistance with even a slight increase in the absolute value of S led to a remarkable average 2.5 times PF improvement. It should be noted that similar PF improvements have been reported by us when combining the same oxide with different liquid or polymer electrolytes[8,9,13] but here this is achieved without the need for an electrolyte. Although variations in the PF are reported here, we would like to mention that the electrical conductivity and the PF values of these oxide films were reported by us previously [130 S m^{-1} and 0.26 μW $(K^2\ m)^{-1}$, respectively],[13] which can be useful in order to establish a meaningful comparison with other materials in the literature.

To evaluate whether the solvent used in the functionalization process (methanol) affects the TE properties of the oxide film, the TE properties of S4, which is the sample immersed just in methanol (without viologen molecules), were also measured (see Table 1). It is clearly observed that there are no significant variations in S and R and, hence, no PF improvement was observed for this sample. Also, to assess the stability of these systems, we measured the Seebeck coefficient and electrical resistance of S3 after one week, obtaining similar results (see Table S1†).

To try to identify the mechanisms behind the variation of the TE properties analyzed, we conducted impedance spectroscopy experiments for S3, before and after its functionalization. The impedance response (see Fig. 5) shows a semicircle in both cases. No additional features appear after functionalization, such as new semicircles, capacitive vertical rises or diffusion (Warburg-like) trends, which leads to the conclusion that the electrical conduction through the film, governed by its ohmic resistance (intercept with the Z' axis) is the dominant mechanism before and after the functionalization. This ohmic resistance decreased from 36.22 kΩ to 20.70 kΩ when the film was functionalized. These values are in good agreement with those provided in Table 1, and we attribute this decrease to a rise in the carrier concentration of the film by the donation of electrons from the viologen molecules upon functionalization. A similar mechanism, but involving electron injection from electrolytes, was also suggested for the same material.[9,13]

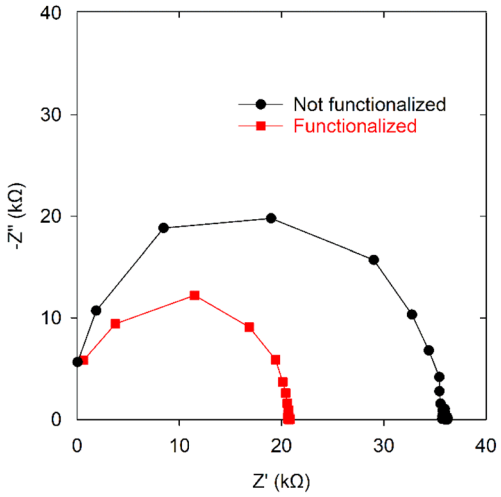

Fig. 5 Impedance spectroscopy response for sample S3 before and after functionalization.

4. Conclusions

We have investigated the variation in the TE power factor of a porous Sb:SnO_2 film after been functionalized with the viologen redox molecule bis-(2-phosphonoethyl)-4,4′-bipyridinium dichloride. It was found that the functionalized film exhibited an average 49.7% reduction in its electrical resistance and an average

8.9% increase in the absolute value of its Seebeck coefficient, leading to a remarkable 2.5 times average PF improvement. Impedance spectroscopy measurements were performed to understand the reasons behind this enhancement. No additional features appeared in the impedance spectrum of the film after functionalization, concluding that an ohmic response is taking place in all cases, with the difference that a higher carrier density exists in the functionalized case due to the donation of electrons upon functionalization. This new approach is of high interest since it improves the TE power factor while decreasing the electrical resistivity and keeping the Seebeck coefficient unchanged (there is even a slight increase), which is uncommon. Its successful application in materials with better TE performance than Sb:SnO_2, which is our future work, could lead to remarkably high power factors and TE performance.

Data availability

Data for this article are available at Zenodo.

Author contributions

M. M. Rahman: writing – original draft, visualization, validation, methodology, investigation, formal analysis. L. Márquez-García: validation, methodology, investigation, supervision. M. Solis-de la Fuente: investigation, supervision. J. García-Cañadas: writing – review & editing, visualization, supervision, resources, project administration, methodology, funding acquisition, formal analysis, conceptualization.

Conflicts of interest

There are no conflicts to declare.

Acknowledgements

This project has received funding from the European Union's Horizon 2020 research and innovation programme under grant agreement no. 863222 (UncorrelaTEd project). Support was also provided by the Conselleria de Educación, Universidades y Empleo of Generalitat Valenciana under the Santiago Grisolia programme (CIGRIS/2021/072).

References

1 M. Luberti, R. Gowans, P. Finn and G. Santori, *Energy*, 2022, **238**, 121967–121984.
2 J. He and T. M. Tritt, *Science*, 2017, **357**, 1369–1379.
3 D. Beretta, N. Neophytou, J. M. Hodges, M. G. Kanatzidis, D. Narducci, M. Martin-Gonzalez, M. Beekman, B. Balke, G. Cerretti, W. Tremel, A. Zevalkink, A. I. Hofmann, C. Müller, B. Dörling, M. Campoy-Quiles and M. Caironi, *Mater. Sci. Eng., R*, 2019, **138**, 210–255.
4 D. Champier, *Energy Convers. Manage.*, 2017, **140**, 167–181.
5 A. R. M. Siddique, S. Mahmud and B. Van Heyst, *Renewable Sustainable Energy Rev.*, 2017, **73**, 734–744.
6 Q. Yan and M. G. Kanatzidis, *Nat. Mater.*, 2021, **21**, 503–513.
7 A. M. Dehkordi, M. Zebarjadi, J. He and T. M. Tritt, *Mater. Sci. Eng., R*, 2015, **97**, 1–22.
8 L. Márquez-García, B. Beltrán-Pitarch, D. Powell, G. Min and J. García-Cañadas, *ACS Appl. Energy Mater.*, 2018, **1**, 254–259.
9 S. Castro-Ruiz, L. Márquez-García, M. Solis-De la Fuente, B. Beltrán-Pitarch, A. Mota-Babiloni, F. Vidan, P. Íñigo-Rabinal, G. Guisado-Barrios and J. García-Cañadas, *Sustainable Energy Fuels*, 2023, **7**, 4254–4259.
10 J. Garcia-Cañadas, F. Fabregat-Santiago, J. Kapla, J. Bisquert, G. Garcia-Belmonte, I. Mora-Seró and M. O. M. Edwards, *Electrochim. Acta*, 2004, **49**, 745–752.
11 K. W. Shah, S. X. Wang, D. X. Y. Soo and J. Xu, *Polymers*, 2019, **11**, 1839.
12 D. Cummins, G. Boschloo, M. Ryan, D. Corr, S. Nagaraja Rao and D. Fitzmaurice, *J. Phys. Chem. B*, 2000, **104**, 11449–11459.
13 M. Solis-De la Fuente, S. Castro-Ruiz, L. Márquez-García, P. Rullière, S. Fantini, R. Del Olmo, N. Casado and J. García-Cañadas, *Sustainable Energy Fuels*, 2025, **9**, 1217–1224.